The Met.Office

Turbulence and Diffusion Note No. 268

FIELD MEASUREMENTS AND MODELLING OF URBAN METEOROLOGY IN BIRMINGHAM, UK

by

N. L. Ellis and D. R. Middleton

20th September 2000

Public Met. Service Research
The Met. Office
London Road
Bracknell
Berkshire, RG12 2SZ

FIELD MEASUREMENTS AND MODELLING OF URBAN METEOROLOGY IN BIRMINGHAM, UK

N. L. Ellis and D. R. Middleton

ABSTRACT

Two four-week urban field campaigns were carried out in spring 1998 and winter 1999. This report presents a comparison of the urban measurements with (i) nearby rural synoptic station observations, (ii) output from The Met. Office Unified Model (UM) and (iii) a Surface Energy Balance model (SEB). Urban wind speeds at 30m were found closest to rural 10m wind speeds; the local urban roughness length was ~0-2m. The urban temperature was ~1°C greater than the rural temperature, with some lag. The UM results showed it models well for a rural synoptic station but the character of the urban site was not captured. The SEB results had good agreement with urban measurements for radiation terms and temperature but showed problems in modelling urban heat flux and stability. A planned urban field campaign for 2000 will seek to (i) gain summer measurements, (ii) gain greater height and (iii) measure additional parameters. It is recommended that long-term routine measurements be initiated in urban areas.

1. Introduction

With nearly half of the world's population living in urban areas (Fenger, 1999), air quality in cities is of increasing concern due to its impact on public health and the environment.

The stability of the atmosphere and local advection are primary in determining the dispersion of pollutants, by controlling the intensity of turbulence and the depth of the surface mixed layer. An unstable atmosphere favours vertical air currents, whereas a stable atmosphere strongly resists upward vertical motions. Consequently pollutants released into a stable atmosphere tend to spread horizontally rather than mix vertically, which can be harmful to life at the surface.

In urban areas advection over increased surface roughness creates greater mechanical turbulence. Stability is further influenced by the urban heat island and its effect on thermally induced turbulence, which may lead to a delay in the onset of the evening transition to night time stable conditions (Middleton, 1998). In the case of a large city these effects can lead to an almost complete absence of stable conditions, which would be present in the surrounding rural areas (Oke 1990), and this will have an effect on air quality.

However, the parameterisation of urban meteorology is not well understood. In order to develop urban dispersion models this must be remedied, particularly the diagnosis of stability over a town or city. Observations play a large part in developing this understanding.

Urban measurements have been collected and (i) compared with nearby synoptic rural data, (ii) compared with analyses from The Met. Office Unified Model and (iii) used to validate, with the aim of developing, a Surface Energy Balance model (SEB). The work described here is based upon short, intensive, field detachments.

The purpose of this study is to increase our understanding of urban meteorology, with the ultimate aim of providing an improved assessment of urban boundary layer stability, which could lead to better air quality forecasts.

2. Urban Measurements

During April/May 1998 and January/February 1999, Meteorological Research Unit (MRU) Cardington carried out two four week measurement campaigns. The location was an industrial site in Birmingham, UK, a city of approximately 1 million inhabitants.

The measurement site was a small grassy area within Dunlop Tyres Ltd., a factory complex in the northeastern sector of the city, in an area of mixed industrial and residential buildings (Figure 1). The M6 motorway lies approximately 0.7 km to the south, running east-west (Rooney, 2000).

The grass site is rectangular in shape with an overall size of approximately $100m \times 50m$, though only $55m \times 40m$ of this is realistically useable. Aerial photographs of the factory are shown in Figures 2 and 3. Note, that there has been some minor development of the site since these photographs were taken in 1992 (see Rooney, 2000).

The 1998 field detachment covered the period 03-04-1998 to 10-05-1998 and the 1999 field detachment ran from 16-01-1999 to 15-02-1999. Instrument masts of $30m$ and $15m$ were used in 1998, and $45m$, $30m$ and $15m$ masts in 1999. At mast heights, measurements were taken of turbulence, wind and temperature. Derived from these were sensible heat flux, friction velocity, roughness length and Monin-Obukhov length. Shortwave and longwave radiation, surface and subsurface temperatures, pressure, rainfall and humidity were also measured. Appendix A gives a full list of instrumentation and measured meteorological variables from the two detachments, (produced by Dave Bamber, MRU Cardington).

3. Data Processing by MRU Cardington

Data from the Dunlop site was logged continuously at $4Hz$, from which hourly averages were obtained. The only exception to this was subsurface temperature, which was logged at 2-minute intervals. Logging and processing of the data was carried out by MRU Cardington and the formulae used for calculating the variables not directly measured at the site are given below.

It is conventional to write the mean of a quantity, u, as $\overline{u}$ and the fluctuation, the deviation from the mean, as u', so that

$$\overline{u} = \frac{1}{n}\sum_i u_i \tag{1}$$

$$\text{and} \qquad u' = u - \overline{u}. \tag{2}$$

Where u, v and w are orthogonal wind speed components, wind speed and direction in the usual convention are derived from $\sqrt{u^2 + v^2}$ and $tan^{-1}\left(v/u\right)$ respectively (with allowance for anemometer alignment and conversion to degrees clockwise from North).

Friction velocity, u_*, quantifies the turbulent velocity fluctuations in the air, where,

$$u_* = \left(\overline{u'w'}^2 + \overline{v'w'}^2\right)^{1/4}. \tag{3}$$

The eddy correlation method is used to calculate sensible heat flux, H, such that,

$$H = \rho c_p \overline{w'T'}, \tag{4}$$

where T' is the fluctuation of temperature and $\overline{w'T'}$ is the covariance of w' and T', ρ is air density and c_p is the specific heat of air at constant pressure.

This approach can only be used if w' and T' can be measured directly. Fast response instruments are needed and the signals must be sampled and averaged sufficiently rapidly. The ultrasonic anemometers deployed at the Dunlop factory can record all of the quantities u', v', w' and T' as required.

To determine boundary layer stability the Monin-Obukhov length (L) is calculated, it being a measure of the relative importance of buoyancy forces to shear effects in turbulence production.

$$L = \frac{-u_*^3}{\left(\frac{k}{30}\right)\overline{w'T'}} \qquad \text{where} \quad \left(\frac{k}{30}\right) \approx \left(\frac{kg}{T}\right), \tag{5}$$

$k \approx 0.4$ is the von Karman constant and g is acceleration due to gravity. The factor 30 arises from assuming $T \sim 300K$ and $g \sim 10 ms^{-2}$.

Roughness length, z_0, is defined such that $u=0$ at height $z = z_0 + \delta$, where δ is the zero-plane displacement height. A stability function, $\Psi(z/L)$, is included for arbitrary boundary layer stability and z_0 is obtained by solving the following,

$$\frac{uk}{u_*} = \ln\left(\frac{z-\delta}{z_0}\right) - \Psi\left(\frac{z}{L}\right), \tag{6}$$

where, for $z >> z_0$, following Oke (1990),

$$\Psi\left(\frac{z}{L}\right) = \begin{cases} -5\, z/L & z/L \geq 0 \\ \ln\left[(1+x^2)(1+x)^2\right] - 2\tan^{-1} x + \left(\frac{\pi}{2} - \ln 8\right) & z/L < 0, \end{cases} \tag{7}$$

where $x = (1 - 15\, z/L)^{1/4}$, (Rooney, 2000).

Finally, given that incoming and outgoing shortwave radiation and net longwave radiation are measured, net radiation can be obtained by,

$$R_{net} = S_{net} - L_{net} = S_{\downarrow} - S_{\uparrow} - L_{net} \tag{8}$$

4. Analysis of Urban Measurements

Figure 4 shows the land use over a $4km \times 4km$ area centred on the Dunlop site (Rooney, 2000). The predominant land use types are defined as continuous urban and suburban. However, even considering the surrounding land use, the most important question is whether the Dunlop site is sufficiently urban to produce representative urban measurements.

To assess the site, Dunlop observations of wind speed and temperature have been compared with corresponding data from nearby Coleshill synoptic station, an exposed rural site situated on farmland on the eastern edge of Birmingham approximately $9km$ to the south east of the Dunlop factory. Figure 1 indicates the relative positions of the two sites. The co-ordinates of the Dunlop factory are 52°31′N and 1°49′W and the co-ordinates of Coleshill synoptic station are 52°29′N and 1°41′W.

In addition, Met. Office Unified Model (UM) analyses for the 1999 measurement period were compared with both the urban and rural observations of wind speed, temperature and, from Dunlop only, sensible heat flux. UM data for each of the Dunlop factory and Coleshill was obtained.

For reference, all Dunlop and Unified Model values are hourly averages. Coleshill observations are made on the hour with wind speeds being an average taken over the preceding 10 minutes and temperatures being spot values.

Note that $30m$ data from the 1999 Dunlop detachment is not discussed here as it had to be disregarded because of instrument problems.

4.1 Dunlop observations versus Coleshill observations

4.1.1 Wind speed

A power law wind profile can be described by an exponent, p, where

$$\frac{u_1}{u_2} = \left(\frac{z_1}{z_2}\right)^p . \tag{9}$$

Jones et al. (1971) recall that, in open country, earlier studies found $p \sim 1/7$ (i.e. 0.143), whilst their results over Sefton Park in Liverpool (ibid, Table 1) produced a range for p of 0.17-0.51. For dry adiabatic lapse conditions they found $p = 0.21$ in an urban environment.

Wind speed at the Dunlop site clearly increased with height (Figures 5a and 5b) and, using the Dunlop wind data from $15m$ and $30m$ from 1998 and $15m$ and $45m$ from 1999, p was found to be approximately 0.35. Note, though, that Jones et al. (1971) used a tethered balloon over a larger height interval than that at Dunlop.

There was also an obvious slowing of the Dunlop wind compared to that at Coleshill.

- Dunlop $15m$ winds (D_{15}) were slower than Coleshill $10m$ (C_{10}) winds (Figures 6a and 6b) by approximately 20%:

  $C_{10} \approx 1.18 \times D_{15}$ (1998 data)

  $C_{10} \approx 1.24 \times D_{15}$ (1999 data)

- Dunlop $30m$ winds (D_{30}) were comparable to Coleshill $10m$ winds (Figure 6c) within approximately 5%:
  $C_{10} \approx 0.95 \times D_{30}$ (1998 data)
- Dunlop $45m$ winds (D_{45}) were faster than Coleshill $10m$ winds (Figure 6d) by approximately 20%:
  $C_{10} \approx 0.82 \times D_{45}$ (1999 data)

In addition, mean wind speed was calculated and the findings were found to be consistent with those above.

	Dunlop				Coleshill	
	15*m*		30*m*	45*m*	10*m*	
	1998	1999	1998	1999	1998	1999
Mean Wind Speed (ms^{-1})	3.5	3.3	4.3	5.0	4.1	4.1

This slowing of the urban wind was almost certainly due to greater surface roughness at the Dunlop site. In analysing the $45m$ factory measurements, Rooney (2000) found that, although with some scatter, the mean roughness length (z_0) increased as the fraction of upwind urban and suburban cover increased, and calculated z_0 to be mostly in the range 0-$2m$.

Steinecke (1999) also found a decrease in wind speed as the level of urbanity increased in Reykjavík. Steinecke's mean wind speed in the city centre was $1.8ms^{-1}$ compared to $2.6ms^{-1}$ in a city park and $4.0ms^{-1}$ on the city outskirts.

4.1.2 Temperature

There is a clear difference in air temperature (measured at ~$1.25m$) between the urban and rural sites. Each plot in Figure 7 is a mean 24-hour period of air temperature calculated over the whole measuring period.

1999 winter data showed the Dunlop factory to be an almost constant 1°C warmer than Coleshill (Figure 7b). This difference was less distinct during daytime for spring 1998 data, but was still evident at night (Figure 7a). This finding is consistent with the idea of an urban heat island. Figure 7 also shows the rural temperature curve slightly lagging that of the urban temperature.

4.2 Observations versus Unified Model

Mesoscale Unified Model (UM) analyses were used here for comparison against the urban and rural observations. Resolution of the UM was approximately $17km$ for the 1998 data and $12km$ for the 1999 data. Data from the nearest grid points were interpolated to obtain values for the Dunlop (UM_D) and Coleshill (UM_C) sites.

4.2.1 Wind speed

The UM_C $10m$ wind speed showed good agreement with the rural Coleshill

observations (Figure 8a), but UM_D $10m$ wind speed was faster than the $15m$ urban Dunlop observations (Figure 8b).

- $UM_C \approx 0.97 \times C_{10}$
- $UM_D \approx 1.2 \times D_{15}$

Comparing the UM analyses for the two grid points found the two to be almost identical (Figure 8c).

- $UM_C \approx 1.04 \times UM_D$

Mean wind speeds were again calculated. Mean UM_C wind speed was found to be $4.2ms^{-1}$ and mean UM_D wind speed was $4.1ms^{-1}$. These values reinforce the above results by being comparable with Coleshill 10m winds and notably faster than the Dunlop 15m winds (Section 4.1.1).

4.2.2 Temperature

UM analyses of temperature showed the Coleshill observations and UM analysis for Coleshill to be in fairly good agreement (Figure 9a), but the Dunlop temperature measurements were consistently higher than the UM analysis for the Dunlop site (Figure 9b). Again, the two UM analyses were found to be in excellent agreement with each other (Figure 9c).

4.2.3 Sensible Heat Flux

Figure 10 presents scatter plots of sensible heat flux from both 1998 and 1999 Dunlop data sets and from the UM for the 1999 period. Overplotted are mean diurnal cycles calculated by averaging over the whole of each measuring period.

Figures 10a and 10b show the 1998 Dunlop $15m$ and $30m$ measurements respectively. Figures 10c and 10d show the 1999 Dunlop $15m$ and $45m$ measurements respectively. Significantly, both sets of $15m$ measurements are positive over 70% of the time, the $30m$ measurements approximately 75% of the time and the $45m$ measurements approximately 55% of the time. These positive values, and the mean diurnal cycles, indicate that the boundary layer is, for the majority, neutral to unstable. In particular, nighttime values are not predominantly negative, implying that a stable nighttime boundary layer is not typical for this site.

Figure 10e shows UM heat flux for the Dunlop site. The UM heat flux goes positive during only one night and this is clearly reflected in the mean diurnal cycle. Values are negative approximately 80% of the time. The UM produces a very idealised diurnal cycle, with the boundary layer stable through the night and unstable in the middle part of the day only. This is typical of a rural boundary layer.

Even though measurements from Coleshill are unavailable for comparison, though planned for a summer 2000 campaign, the UM heat flux for Coleshill was obtained (Figure 10f). The two UM analyses are almost identical.

The implied stability difference between the UM analyses and the Dunlop observations is consistent with the expected contrast between urban and rural sites (Oke, 1990). The almost exact match of the two UM analyses again shows a lack of urban consideration within the UM.

4.3 Summary

Slower wind speeds are observed at the urban Dunlop site compared to the rural Coleshill measurements, and temperatures are consistently slightly higher at Dunlop, particularly at night. The differences between the two sets of measurements indicate clear urban effects evident in the Dunlop measurements.

UM output for Coleshill matches observations from the exposed rural site well. However, UM output for the Dunlop site shows little agreement with the urban observations. The two UM analyses were almost identical. These findings suggest a lack of urban consideration within the UM and that the character of the Dunlop site, and thus the rural-urban contrast, was not modelled.

5. Surface Energy Balance (SEB) Model

The POST model (POrtable Surface Temperature) was developed by Best (1998) and adapted by him to produce the Surface Energy Balance model (SEB) used here. SEB (i) couples a canopy to the ground solely by radiation, (ii) solves the heat transfer equations in the soil or concrete below the surface and (iii) calculates the energy balance in the atmospheric surface layer as a function of atmospheric stability. The model uses an iterative process to estimate an initial soil temperature profile. Figure 11 illustrates the energy balance terms used in the model.

Simple parameterisations are used within SEB so that it can be run on standard synoptic meteorological data, thus allowing it to be portable. The model is run on two input data files. The first contains hourly synoptic data of air temperature, dew point temperature, pressure, wind speed at $10m$, total, low, medium and high cloud amounts and precipitation amount. The second file contains values relating to properties of the canopy and underlying surface as well as the latitude and longitude of the site being considered.

Output parameters from the model are shortwave radiation, incoming longwave radiation, outgoing longwave radiation from the canopy, outgoing longwave radiation from the ground, sensible heat flux, latent heat flux, ground flux, the reciprocal of the Monin-Obukhov length, friction velocity, surface temperature and subsurface temperature.

SEB was designed to be run for rural areas (homogeneous surfaces) but this study assesses the potential for adapting it to urban areas by implementing a concrete, rather than vegetation, canopy. This is achieved by changing certain values in the surface properties input file to being appropriate for concrete rather than vegetation. Table 1 shows these values for both types of canopy.

6. Data Collection Problems

During field detachments, problems with instrumentation or data logging, for example, can easily lead to the loss of observational data. When data is missing for a single hour continuity is assumed to fill in the gaps, as the SEB model requires continuous hourly data for input. However, if data is lost for longer periods these hours are ignored and SEB is run up to and from after the data gap.

There have been two major instances of data loss. Logging was halted for a week during the 1998 detachment due to a blown fuse and, therefore, the data from May 1998 has been disregarded. During the 1999 detachment almost three days of

data, 9-02-1999 to 11-02-1999 inclusive, was lost due to a disk malfunction. In addition, as stated previously, all data from the $30m$ ultrasonic anemometer had to be disregarded from the 1999 detachment because of problems with the instrument. However, a total of 23 days of useable data is available from 1998 and 25 days from 1999.

In addition, due to fewer instruments being deployed during the first detachment in 1998, pressure, dew point temperature and precipitation are missing from this data set. Cloud cover amounts were unable to be recorded at the site during either detachment. Section 7 discusses how this data was obtained by other means.

The radiation balance meter was not able to measure separate incoming and outgoing longwave radiation, as needed for full model validation, as the temperature of the instrument was not known. Only *(incoming longwave – instrument temperature)* and *(outgoing longwave – instrument temperature)* could be measured, though net longwave radiation could be deduced from these,

$$\left(L_{\uparrow} - T_{instrument}\right) - \left(L_{\downarrow} - T_{instrument}\right) = L_{\uparrow} - T_{instrument} - L_{\downarrow} + T_{instrument} = L_{\uparrow} - L_{\downarrow} = L_{net}$$

No humidity measurement was taken in 1998, and in 1999 only a slow response instrument was available. Consequently, measurements could not be taken frequently enough to be able to calculate $\overline{w'q'}$, which would be needed in order to calculate latent heat flux using the eddy correlation method. Furthermore, humidity was only measured at one height in 1999 and so latent heat flux could not be calculated using a humidity gradient either. Therefore, measurements of latent heat flux and, hence, ground flux were not obtained. Ground flux being unobtainable because it was not measured directly and latent heat flux would be needed to determine it indirectly.

7. Retrieval of Synoptic Meteorological Data

7.1 Data Retrieval

As stated in Section 6, not all of the required data was measured at the Dunlop site. The missing data needed for SEB model input consisted of cloud cover amounts (low, medium, high and total) for both detachments, as well as precipitation, dew point temperature and pressure for the 1998 detachment. Data was retrieved from the Met. Office's meteorological database, from Coleshill synoptic station records, to complete the two data sets.

Precipitation amounts for the 1998 detachment turned out to be unavailable from the database. Therefore, observed, hourly past and present weather codes were retrieved instead. From these the occurrence, or not, of precipitation could be inferred by manual analysis. This was sufficient for our purposes as SEB requires this only, not the amount of precipitation.

Pressure and dew point temperatures for the 1998 period were both obtained from the database with no retrieval problems.

Only C_T (total cloud) and C_L (low cloud) data could be retrieved directly. It was necessary to determine C_M (medium cloud) and C_H (high cloud) from coded 8 groups, again by manual analysis, which provide cloud type, amount and base height. However, rules followed when recording this information could mean a large amount of data has been disregarded.

Not all individual cloud has to be recorded, which means that C_T is sometimes greater than the sum of C_L, C_M and C_H. Also, if no low cloud is present but there is medium cloud, C_M can be recorded in the C_L column, as it is the dominant cloud group. Close examination of the 8 groups is needed to determine if this has occurred to avoid mixing the two cloud types.

7.2 Suitability of Synoptic Data

Section 4 describes many significant differences between measurements taken at Dunlop Tyres Ltd. and Coleshill and, not unexpectedly, potentially large differences in the cloud cover are discussed here.

On most occasions the SEB model calculates the magnitude of net solar radiation quite accurately, but there are also instances of the magnitude being modelled poorly. An example of this is given in Figure 12a, which compares Dunlop measurements and SEB output for 22 January 1999, though unfortunately hour 1300 is missing from the Dunlop data on this day. Note that this day had a high pollution episode and there was an occurrence of fog, with the meteorological database records showing the fog present at Coleshill. However, someone closer to the Dunlop site noted that it had been a very clear day (Bob Appleby, personal communication), this probably being due to heat from the city and consistent with urban effects. Recall that Coleshill cloud data is used in SEB, and so when total cloud cover for part of this day is changed from complete to none, the magnitudes of SEB modelled and Dunlop measured net shortwave radiation become in much better agreement (Figure 12b).

Tests using Dunlop measured incoming shortwave radiation as a model input have shown that if this parameter is correct then modelled net shortwave radiation is in very good agreement with that measured. This implies that it is the model calculation of incoming shortwave radiation that harbours the problem. The main parameters in this calculation are solar elevation and total cloud amount. We can assume that the formula for solar elevation is correct, thus implying the value given to total cloud amount regulates the accuracy of model shortwave radiation.

Total cloud amounts could be adjusted such that SEB modelled and Dunlop measured net shortwave radiation are in agreement, though this would be very time consuming and has not been carried out. However, this could only be implemented during daylight hours. At night, when there is no incoming shortwave radiation, there is no way of checking the accuracy of the cloud data. In addition, this only validates total cloud amount. The model calculation for shortwave radiation does not depend on separate low, medium and high amounts and, therefore, we have no way of amending these.

As stated previously, Section 4 emphasises the differences between meteorological conditions at Coleshill and Dunlop Tyres Ltd., as do the findings in this section. Applying rural Coleshill data to the urban Dunlop site is not desirable, but most of the measurements not taken at Dunlop are essential input for the SEB model. Coleshill is the closest synoptic station to Dunlop and its records provide the only way to complete the Dunlop data sets. Therefore, for this report, only the 1999 Dunlop data will be used for input and validation of SEB. Only cloud cover amounts are required to complete this data set and, despite the uncertainties with the Coleshill cloud data, SEB radiation is well enough predicted, as will become clear.

8. SEB Model Analysis

8.1 Stability diagnosis

A significant problem identified for this particular study is that, on a number of occasions, the SEB model determines the boundary layer to be very stable and does not calculate $1/L$ because it deems Monin-Obukhov theory no longer valid. This assignment of model stability is very much in disagreement with the urban measurements, which indicate the boundary layer to be neutral or near neutral for the majority of the measuring period. Figure 13a shows SEB calculated $1/L$ against the Dunlop $15m$ measurements. Due to some large values it is difficult to compare the two data sets near zero, so Figure 13b shows this data with an adjusted y-axis range.

For the majority, the two sets of data are of opposite sign. Also, there are large gaps in the SEB output where the model does not calculate a value for $1/L$, though the implication is that it would be very large positive if it were calculated. The most notable occurrences of this are 21-23 January, 29 January-3 February and 12-13 February. During these periods a number of other modelled variables appear to be detrimentally effected (not shown), though they are often in very good agreement with the urban measurements at all other times.

The effect on the other modelled variables occurs through the direct dependence of u_* and aerodynamic resistance (r_a) on $1/L$, as the model calculations for u_* and r_a include the stability function $\Psi(z/L)$, (Equation 7, Page 3). The largely incorrect modelled values of $1/L$ cause large errors in the value given to the stability function, which are then passed on throughout the rest of the model.

A test was performed in which the stability dependence was removed by estimating u_* and r_a assuming neutral stratification, which effectively means setting $1/L$ to zero in $\Psi(z/L)$. As an example, Figures 14a and 14b show u_* modelled in both ways, with Dunlop measurements overlaid, for six days that were notably effected by the aforementioned problem.

In the case where u_* and r_a are stability dependent (Figure 14a), Monin-Obukhov theory is deemed invalid for the majority of the six days. This is because the modelled value of $1/L$ becomes very large before reaching a cut off value, which causes a very small u_* to be returned. By removing the stability dependence (Figure 14b) inappropriate large values of $1/L$ are prevented and the value of u_* stays larger and in good agreement with measurements. Other effected model output also come in to line with the urban measurements in this case.

In addition, because measured stability is near neutral for the majority of the 1999 measuring period, assuming neutral conditions in the model has little significant effect on the previously unaffected time periods. Also, an estimate for $1/L$ can still be calculated later within the model. Therefore, for this report, model results with u_* and r_a estimated using neutral stratification will be those analysed.

However, it is noted that this does not solve the underlying problem. It is simply fortunate that stability during the measuring period was near neutral, so assuming this in SEB was feasible. The question remains as to why the model calculates a very stable boundary layer when this is clearly not correct. This actually stems from problems with modelling sensible heat flux. For this study, SEB modelled

heat flux tends to have the opposite sign to that measured and it is this variable that then determines the sign of $1/L$. This will be discussed in more detail in Section 8.3. In addition, although Monin-Obukhov similarity theory is widely used, its application to urban areas is not necessarily appropriate, especially near buildings.

8.2 Model results

8.2.1 Radiation

Modelled radiation is extremely dependent on the accuracy of the input cloud amounts. Even with questionable cloud data however, the shortwave radiation, both incoming and net (Figure 15a), is modelled extremely well. There is an obvious one-hour lag between the two sets of results, the reason for this is being investigated.

Longwave radiation is very difficult to fully validate. Measurements were obtained of net longwave radiation only, but SEB calculates incoming, outgoing from ground and outgoing from canopy longwave radiation. Net longwave has been added to the model output, but agreement between this and measurements (Figure 15b) does not guarantee the same for the individual terms. In addition, there is still the sensitivity to cloud cover amounts.

However, despite the uncertainties, net longwave radiation actually appears to be modelled fairly successfully, capturing the general pattern well, though there are areas where large errors in magnitude are evident. The majority of these can probably, in part, be put down to cloud inaccuracies.

Figure 15c shows net radiation results. Even considering the problems, it is fair to say that radiation as a whole is modelled fairly successfully.

8.2.2 Surface and subsurface temperatures

For validation of surface and subsurface temperatures SEB has been run in two ways, using both concrete and vegetation canopies. This is because only grass surface and 1m deep soil temperatures were measured at the Dunlop site. Modelled concrete temperatures would not be entirely compatible with the measurements so it would be unfair to assess the model on these alone.

The concrete canopy surface temperature curve is slightly smoother than that of the measured values (Figure 15e) and it does not cool as much some nights. The vegetation canopy results show more detail (Figure 15d), i.e. this surface responds quicker to temperature changes, and achieve a much better fit to the observed data. The better agreement of the vegetation temperature with Dunlop measurements is no surprise because of the surface the measurements were taken from, but it does stress the need for concrete temperatures from future measurement campaigns. However, the model results for surface temperature are extremely encouraging whichever model run is chosen.

For subsurface temperature, surprisingly, the magnitude of the concrete canopy results (Figure 15g) is better than that of the vegetation canopy (Figure 15f). However, a problem with both sets of data is caused by the model's initial value being far too large. This affects the general pattern of the curves as it seems the model takes some time to settle after this high first value, with the concrete canopy run suffering the most of the two. The SEB model uses an iterative process to achieve a first value for the subsurface temperature so it may be that this needs to be modified.

The concrete canopy fails to pick up a lot of the subtle temperature changes, though this is expected as the measurement has been taken from soil. The vegetation canopy run performs generally better in this respect, but overall there is much room for improvement

8.2.3 Friction velocity

Friction velocity (u_*) is well modelled, as Figure 15h shows, though its magnitude is strongly affected by z_0. Deemed appropriate for an urban area, a constant $1.0m$ has been assigned to z_0 here. This value produces a modelled u_* with good magnitude and overall fit. For reference, measurements of z_0 at the Dunlop site over the four weeks were mostly in the range from 0-2m (Rooney, 2000).

8.2.4 Latent heat flux and ground flux

Both latent heat flux and ground flux were unable to be validated due to a lack of measured data (see Section 6). However, both contribute elsewhere in the model calculations and so validation is essential. These two parameters will be measured in the summer 2000 measurement campaign.

8.2.5 Sensible heat flux

Figures 15i and 15j show Dunlop 45m and 15m sensible heat flux respectively. The two figures clearly show much disagreement between Dunlop measurements and SEB model output. Unfortunately, it does not seem that this can be rectified easily, as discussed in Section 8.3.

8.3 SEB representation of sensible heat flux

A possible reason there is little agreement of sensible heat flux (Figures 15i and 15j) between SEB output and Dunlop measurements is that the two are not entirely compatible. SEB calculates H between the surface (T_S) and $1.25m$ (T_{air}) using a temperature gradient. The sign of modelled H, which effectively determines the stability of the model boundary layer, is decided by $T_S - T_{air}$ alone, with T_{air} a model input and T_S calculated by the model. Dunlop measurements of H are available from 15m and 45m and are calculated by the eddy correlation method (Equation 4, Page 3).

There are two factors noted here that could contribute to the seemingly poor performance of the SEB model. They are area for which the heat flux value is representative of and the method by which it is calculated.

The height at which an instrument is mounted can greatly affect the measurement taken. Schmid and Oke (1990) define the source area as a portion of the upstream "surface area containing the sources and/or sinks which influence those air parcels carried past the sensor under given external conditions." The size of the source area can be affected by stability, turbulence intensity and the measuring height (Schmid, 1994).

As the height of the instrument increases, the 'footprint' that can be seen on the ground grows. As such, a measurement taken very low will represent the

immediate surrounding area, whereas a measurement taken much higher will be representative of a much larger area and will be affected by changes in surface roughness upstream from the measurement site. Claussen (1987) also found that modification of observations could occur if a downstream change in roughness was not a sufficient distance away.

However, rural areas are ordinarily covered by one surface type over a large area and roughness elements are small. The upstream distance to a different surface roughness is usually far enough to ensure that it is the same surface type being represented in measurements at different heights. Therefore, it can be assumed that a constant flux layer exists, with smooth temperature profiles, and a measurement of heat flux at low levels would be expected to be in agreement with the heat flux higher up. This is the type of surface SEB was designed to deal with and is why the model uses a low level temperature gradient to calculate sensible heat flux.

Over an urban site roughness does not remain constant over a wide area. Close to the surface the flow will tend towards equilibrium with the local surface conditions but higher up the flow will be influenced by the different upstream surfaces (Hewer, 1993). Hence, heat flux measurements are taken at greater heights to get a more representative value and eddy correlation is the method used to take the measurements as temperature profiles will deviate and distort in non-homogeneous surroundings.

In essence, there is much less uniformity in urban areas. Some model heat flux error may stem from the fact that the T_S used in the SEB calculation is modelled and will, therefore, contain errors itself. However, even if the Dunlop measured T_S is used within SEB, the modelled heat flux is only improved very slightly, as the problems discussed above are still present.

8.4 Roughness length for temperature

There is some uncertainty, not just with reference to the SEB model but generally, associated with roughness length for temperature, z_{0t}. The common method of determining its value is simply to divide the roughness length for momentum, z_0, by ten. However, it has been suggested, for example by Hewer (1993), that this is incorrect, and z_{0t} could be significantly smaller. This could be important because a change in z_{0t} can affect modelled surface temperature, through the calculation of aerodynamic resistance. If z_{0t} is reduced by an order of magnitude or more, surface temperature can change quite significantly, sometimes improving and other times worsening. Further work is required to determine, firstly, if z_{0t} should be smaller than first assumed and, secondly, if this is the case what value it should be given.

9. Conclusion and Future Work

The main purpose of the West Midlands Urban Meteorology study is towards the improvement of parameterising the meteorology over a city. An improvement by numerical models in forecasting the stability of the urban boundary layer, and thus the dispersion of pollutants, could lead to better air quality forecasts.

Valuable urban data sets have been compiled at Dunlop Tyres Ltd. that exhibit features expected of an urban boundary layer. Comparisons with nearby rural synoptic data show the urban site to be generally warmer and to have slower winds. It is clear also that these urban characteristics have yet to be incorporated into operational numerical weather prediction models, as comparisons against the Unified Model show. Comparisons of heat flux between the Unified Model and Dunlop measurements are particularly interesting for dispersion, with the mean diurnal cycles differing greatly. The assessment of sensible heat flux will be expanded during the 2000 detachment, with it being measured at the rural Coleshill site.

Urban-rural differences between Dunlop Tyres Ltd. and Coleshill synoptic station highlight the need to measure urban meteorology routinely alongside current synoptic observations and air pollution monitoring. This could be in the form of permanent urban synoptic sites. Ideally, sites more representative of urban areas would be preferable, with a denser, more complex building arrangement. Also, an urban synoptic station would have different requirements to a rural station, particularly with respect to the heights at which measurements were to be taken. In addition, if urban data is not available it is just as important to note that using rural data, without modification, for urban purposes should be avoided.

Initial results indicate that the SEB model handles radiation terms, temperature and friction velocity well, but there are significant problems in its prediction of sensible heat flux and Monin-Obukhov length. This is a result of model assumptions of homogeneity that are not appropriate for urban areas. In addition, the model canopy is coupled to the ground solely by radiation. Perhaps the inhomogeneous surface of an urban area requires a more complicated coupling, including heat and moisture transfer. Thus, the SEB model would need considerable development before it could be used for urban applications.

If SEB were to be developed additional validation would be needed, in particular of latent heat flux and ground flux, as the problem with the modelling of sensible heat flux could be being affected by other terms in the model energy balance. In addition, SEB's application of Monin-Obukhov similarity theory to urban areas has not been tested due to the sensible heat flux problems. Note that latent heat flux and ground flux will be measured during the planned summer 2000 campaign.

In view of the capital and resource costs of a comprehensive long-term network or urban meteorology stations, such as turbulence probes, vapour fluxes and remote sensing of wind and temperature profiles, collaboration with other institutions is being investigated. Such collaboration includes bodies in COST715 Action on Urban Meteorology, and UK Universities in the APRIL network (Air Pollution Research in London).

Acknowledgements

My thanks go to colleagues at Meteorological Research Unit, Cardington (D. Bamber, G. Rooney, S. Sewell, T. Jones, J. McGregor, G. Conway and B. Claxton) for carrying out the field detachments and processing the urban data.

Thanks also to Dunlop Tyres Ltd., in particular the assistance of Ian McGregor, for allowing the measurement campaigns to be conducted at their site.

The work was funded by The Met. Office Core and Public Meteorological Service Research programmes.

References

Best, M. J., 1998, 'A model to predict surface temperatures', *Boundary Layer Meteorology*, **88**, 279-306.

Claussen, M., 1987, 'The flow in a turbulent boundary layer upstream of a change in surface roughness', *Boundary Layer Meteorology*, **40**, 31-86.

Fenger, J., 1999, 'Urban air quality', *Atmospheric Environment*, **33**, 4877-4900.

Hewer, F., 1993, 'A roughness length for temperature', *Met. O. (APR) Turbulence and Diffusion Note, No. 208*, The Met. Office, London Road, Bracknell, Berkshire, RG12 2SZ, UK.

Jones P. M., de Larrinaga M. A. B. and Wilson C. B., 1971, 'The urban wind velocity profile', *Atmospheric Environment*, **5**, 89-102.

Middleton, D. R., 1998, 'A new box model to forecast urban air quality', *Environmental Monitoring and Assessment*, **52**, 315-335.

Monteith, J. L. and Unsworth, M., 1990, *Principles of Environmental Physics*, Arnold, pg. 243

Oke, T. R., 1990, *Boundary Layer Climates*, London: Routledge 2nd edition.

Rooney, G. G., 2000, 'Comparison of upwind land use and roughness length measured in the urban boundary layer', *MRU Cardington Technical Note, No. 51*, Met. Research Unit, Cardington Airfield, Shortstown, Bedford, MK42 0TH, UK.

Schmid, H. P., 1994, 'Source areas for scalars and scalar fluxes', *Boundary Layer Meteorology*, **67**, 293-318.

Schmid, H. P. and Oke, T. R., 1990, 'A model to estimate the source area contributing to turbulent exchange in the surface layer over patchy terrain', *Q. J. R. Meteorol. Soc.*, **116**, 965-988.

Steinecke, K., 1999, 'Urban climatological studies in the Reykjavík subarctic environment, Iceland', *Atmospheric Environment*, **33**, 4157-4162.

APPENDIX A

BIRMINGHAM INSTRUMENTATION
Spring (April/May) 1998 and Winter (January/February) 1999

WIND

u,v,w at 30m and 45m*	Ultrasonic anemometers (*Gill Instruments Horizontally Symmetric Research Ultrasonic Anemometer Model No.1199HSH*)
u,v,w at 15m	Ultrasonic anemometer (*Gill Instruments Asymmetric Research Unit Model No.1012R2A*)

TEMPERATURE

At 45m* and 30m	Screened and ventilated PT100 resistance thermometers measured using bridges (*Labfacility Tempmaster 100*)
At 15m	Screened and ventilated PT100 resistance thermometer measured using bridge (*Automatic Systems Laboratories F250*)
At 1.5m	Screened and ventilated PT100 resistance thermometer measured using bridge (*Automatic Systems Laboratories F250*)
On grass surface*	Screened and ventilated PT100 resistance thermometer and temperature transmitter (*HBS 4000-E*)
On concrete slab	Screened and ventilated PT100 resistance thermometer and temperature transmitter (*HBS 4000-E*)
At 1m below surface	PT100 resistance thermometer and temperature transmitter (*HBS 4000-E*)

RADIATION

Net radiation at 15m	Radiation balance meter (*Dr. Bruno Lange GmbH Schulze type Model LXV055*)
Upward and downward short wave radiation at 15m	Pyranometers (*Kipp & Zonen CM21*)

HUMIDITY

Relative humidity at 1.2m*	Dew point hygrometer (*Michell Instruments*)

PRESSURE

At 1m*	Pressure transducer (*Setra Model 270*)

RAINFALL

At ground level*	Tipping Bucket rain gauge (*Met. Office pattern*)

(* indicates not deployed during spring 1998 detachment)

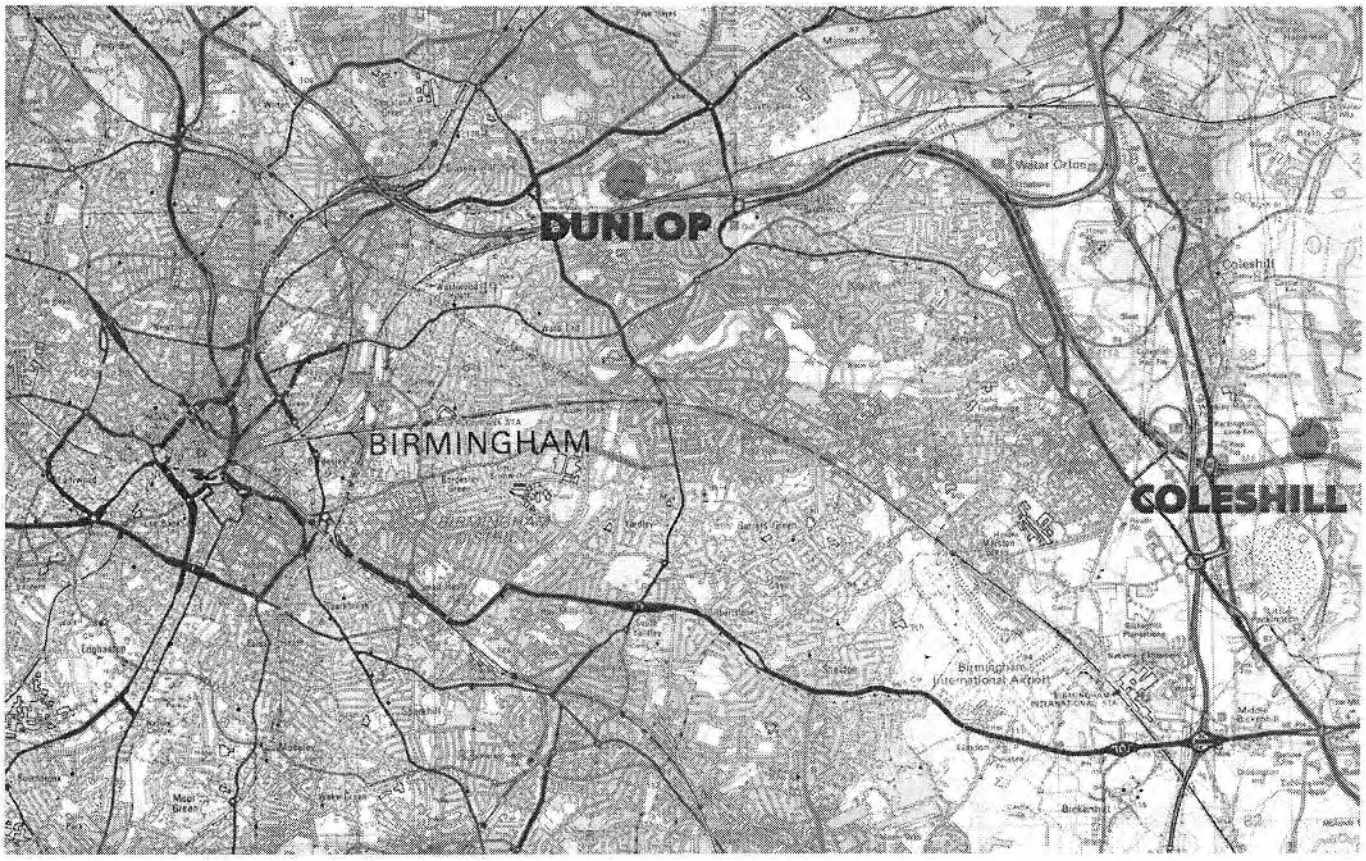

Figure 1: Relative positions of Dunlop Tyres Ltd. and Coleshill synoptic station. Map shows an area of approximately $17.4km \times 10.9km$.

Figure 2: An aerial photograph of Dunlop Tyres Ltd. taken from the west. The measurement site is marked X. (Rooney, 2000)

Figure 3: An aerial photograph of Dunlop Tyres Ltd. taken from the south. The measurement site is marked X. (Rooney, 2000)

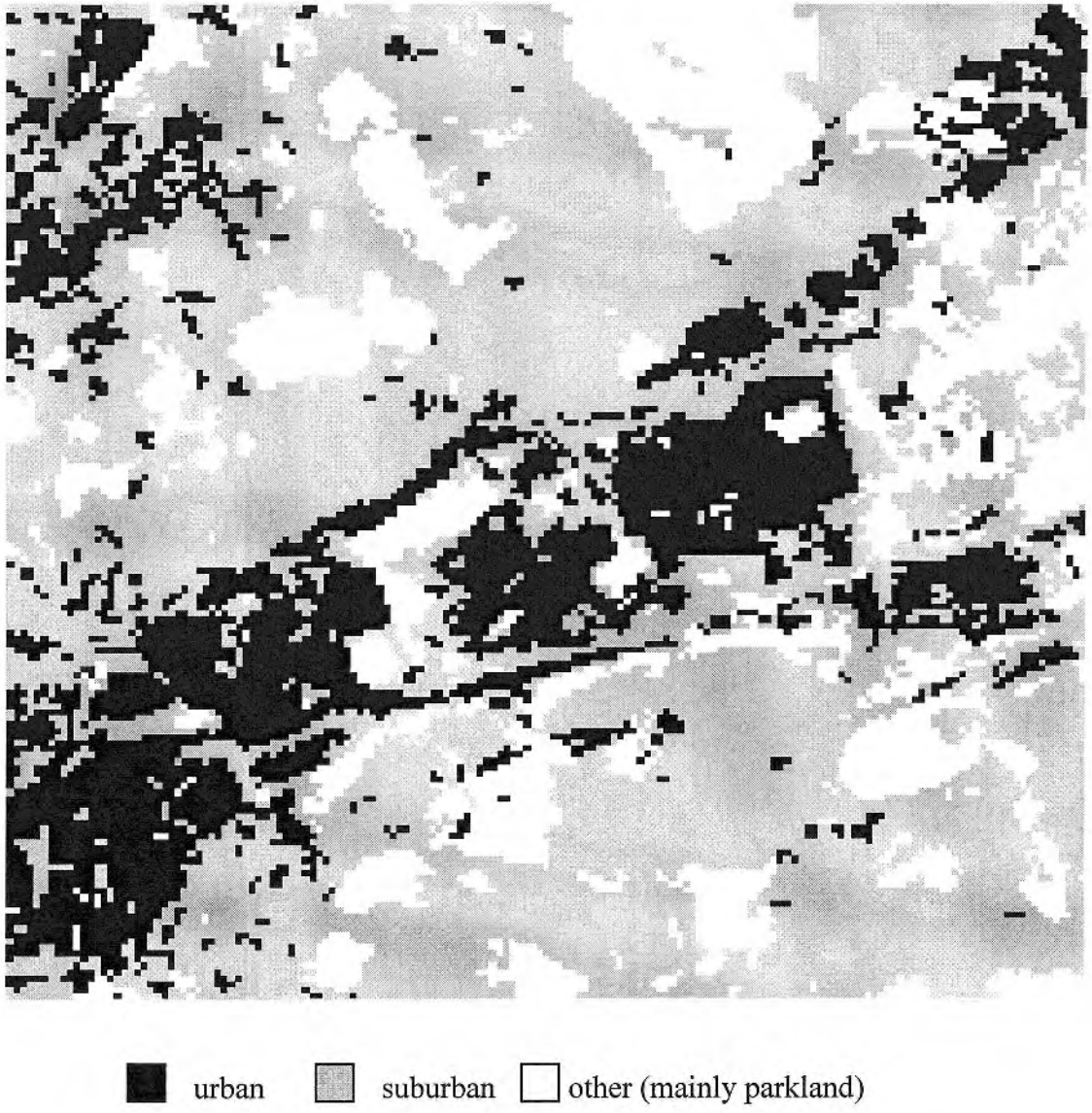

Figure 4: Land cover over a $4km \times 4km$ area centred on Dunlop Tyres Ltd. Pixel resolution is $25m$ and the above key classifies pixels. Data is from the Institute of Terrestrial Ecology, (Rooney, 2000).

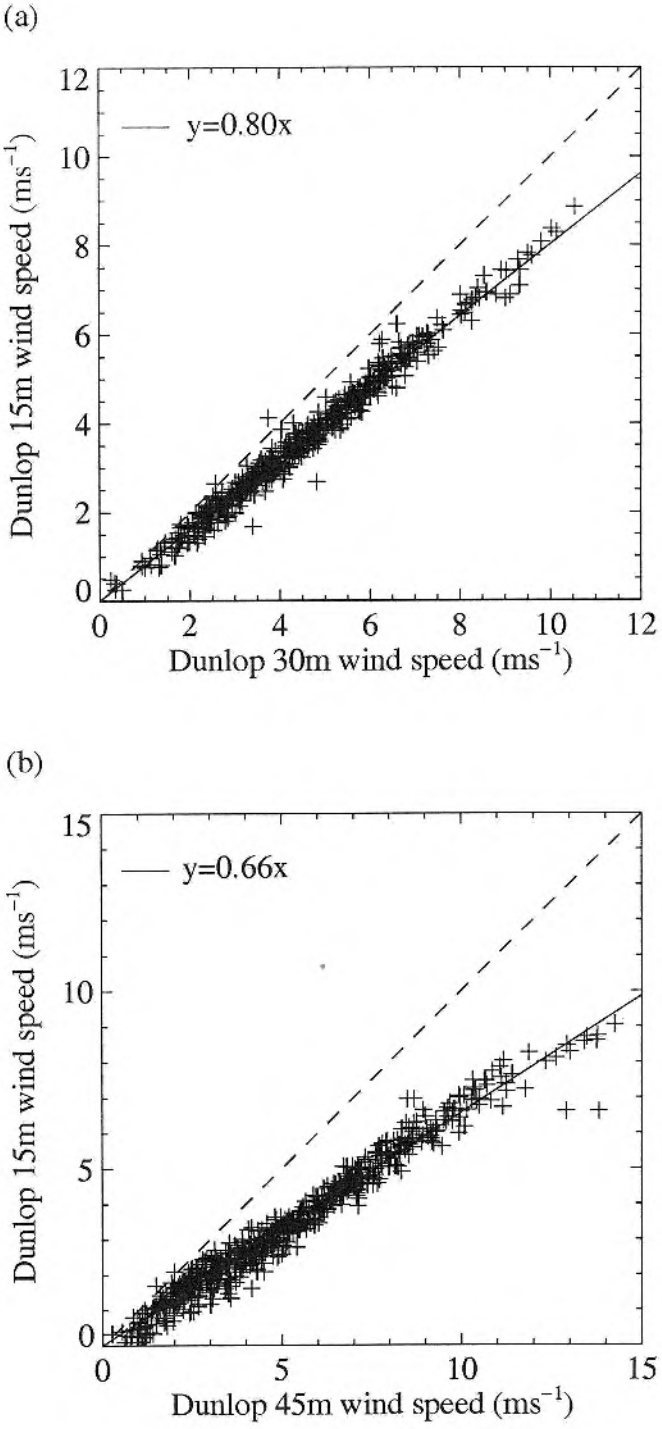

Figure 5: Comparisons of hourly wind speeds at different heights from Dunlop Tyres Ltd.
(a) 30m v 15m, 1998 data and (b) 45m v 15m, 1999 data.
Dashed lines are y=x and solid lines are best fits by least squares method.

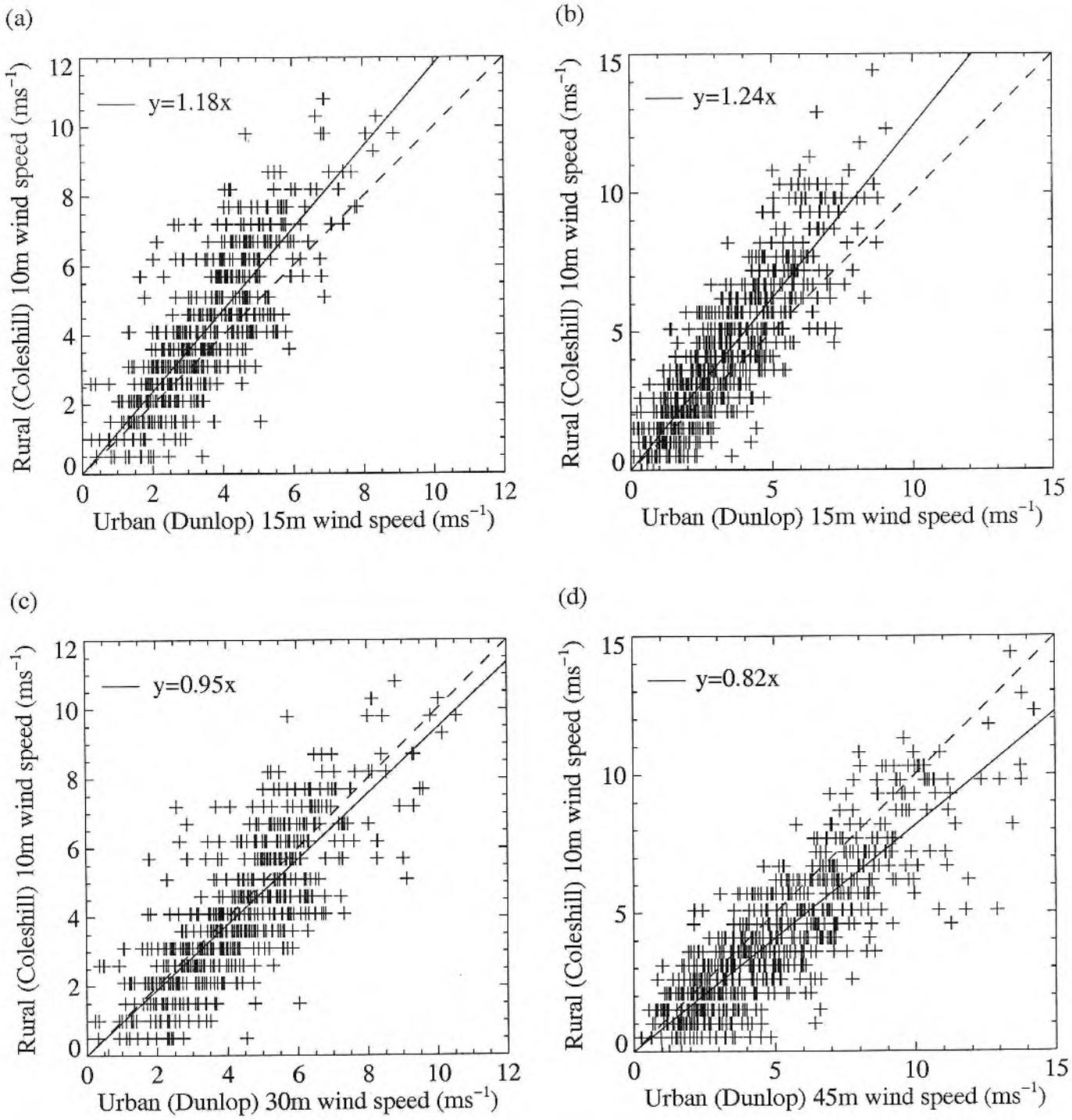

Figure 6: Comparisons of hourly wind speeds from Dunlop Tyres Ltd. (D) and Coleshill synoptic station (C). (a) D 15m v C 10m, 1998 data, (b) D 15m v C 10m, 1999 data, (c) D 30m v C 10m, 1998 data and (d) D 45m v C 10m, 1999 data. Dashed lines are y=x and solid lines are best fits by least squares method.

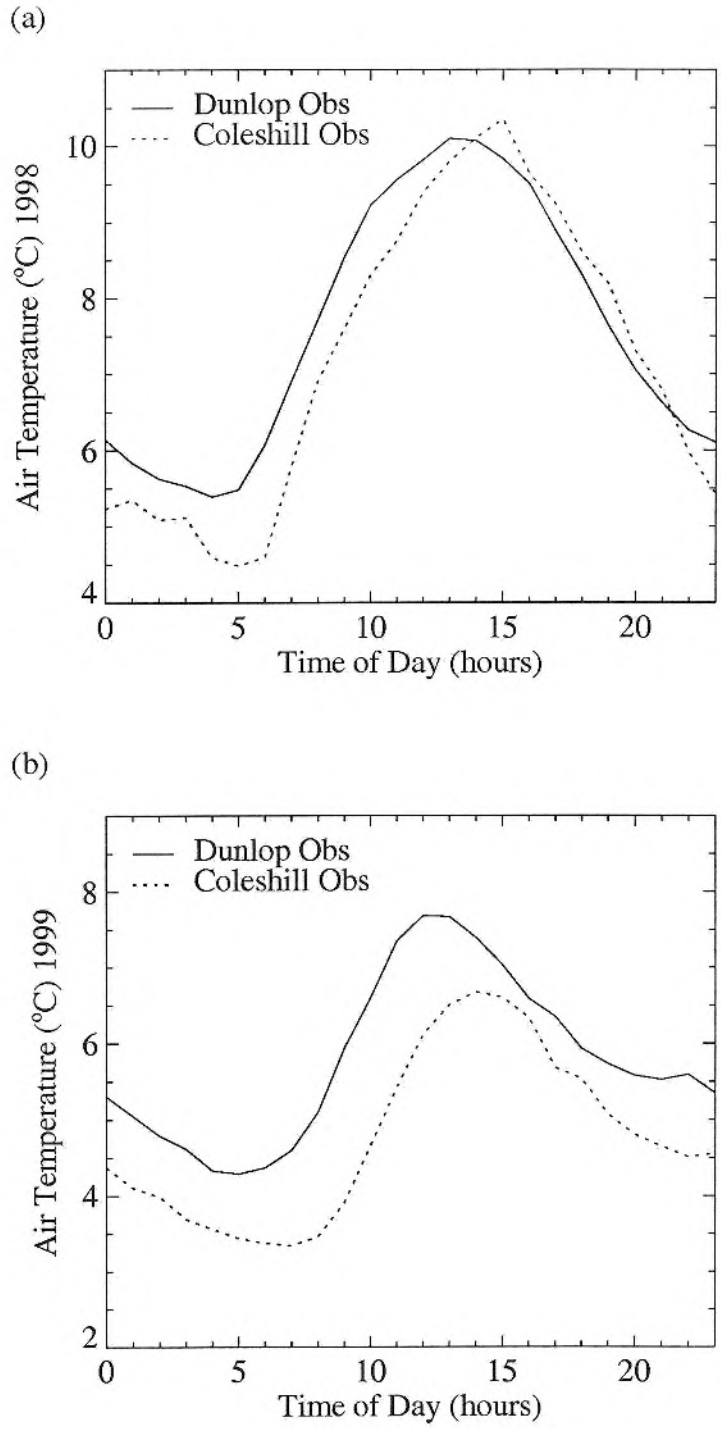

Figure 7: Comparisons of hourly air temperatures, averaged over the measuring period to give a mean 24–hours, from Dunlop Tyres Ltd. and Coleshill synoptic station. (a) 1998 data and (b) 1999 data.

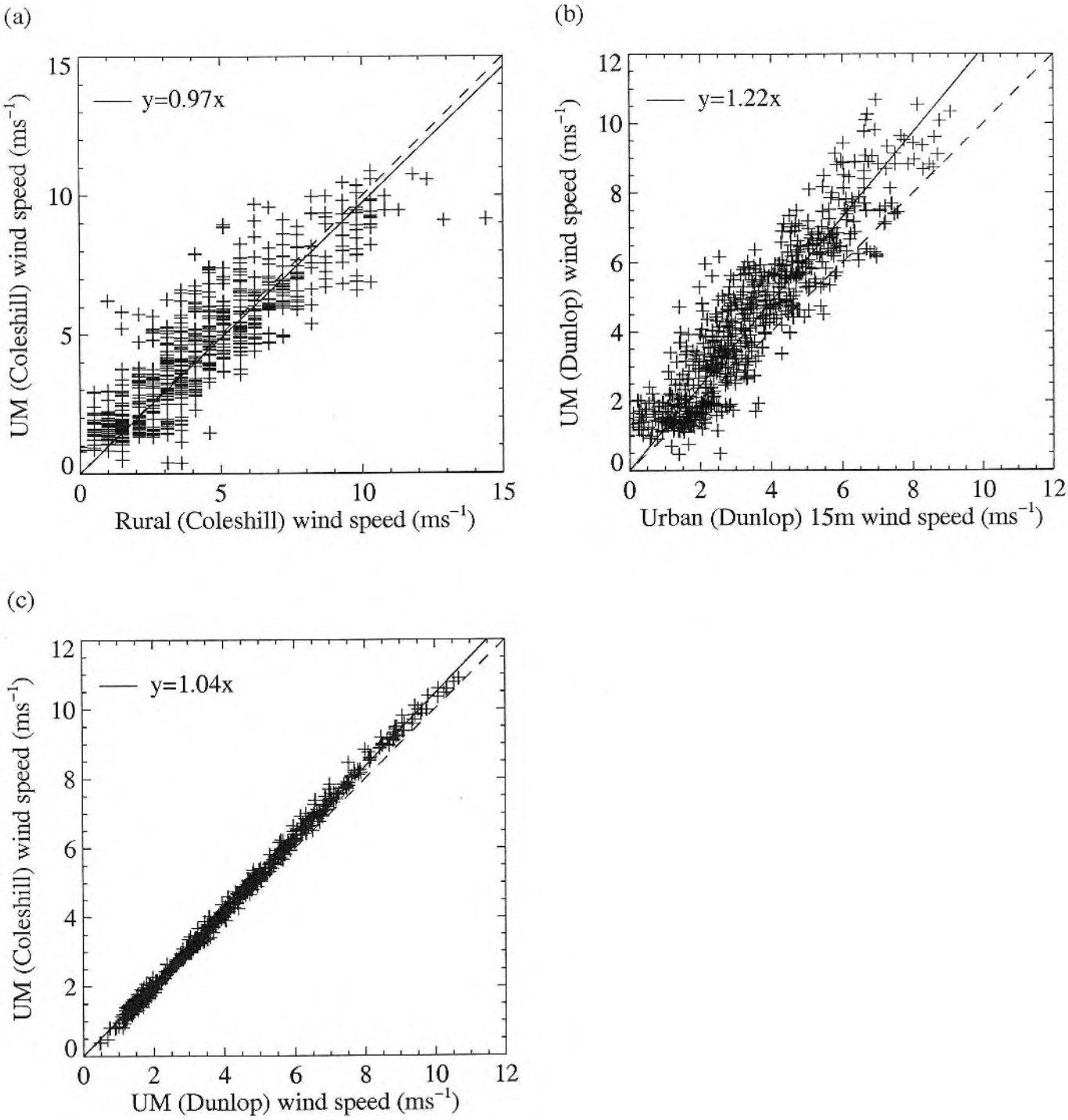

Figure 8: Comparisons of hourly wind speeds from Dunlop Tyres Ltd. (D), Coleshill synoptic station (C) and The Met. Office Unified Model (UMD for Dunlop and UMC for Coleshill).
(a) C 10m v UMC, (b) D 15m v UMD and (c) UMD v UMC. All data is 1999.
Dashed lines are y=x and solid lines are best fits by least squares method.

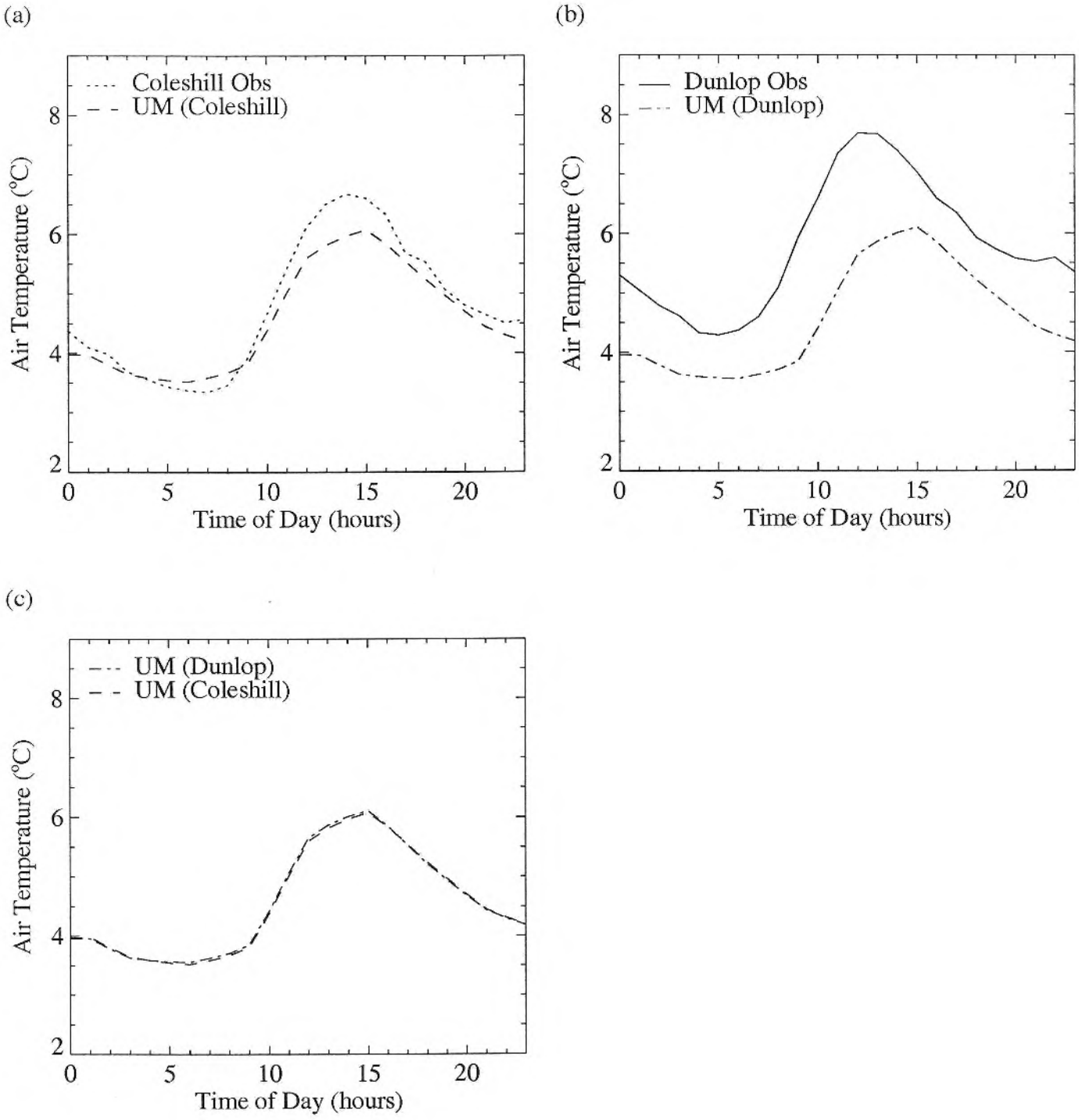

Figure 9: Comparisons of hourly air temperatures, averaged over the measuring period to give a mean 24–hours, from Dunlop Tyres Ltd., Coleshill synoptic station and The Met. Office Unified Model. All data is 1999.

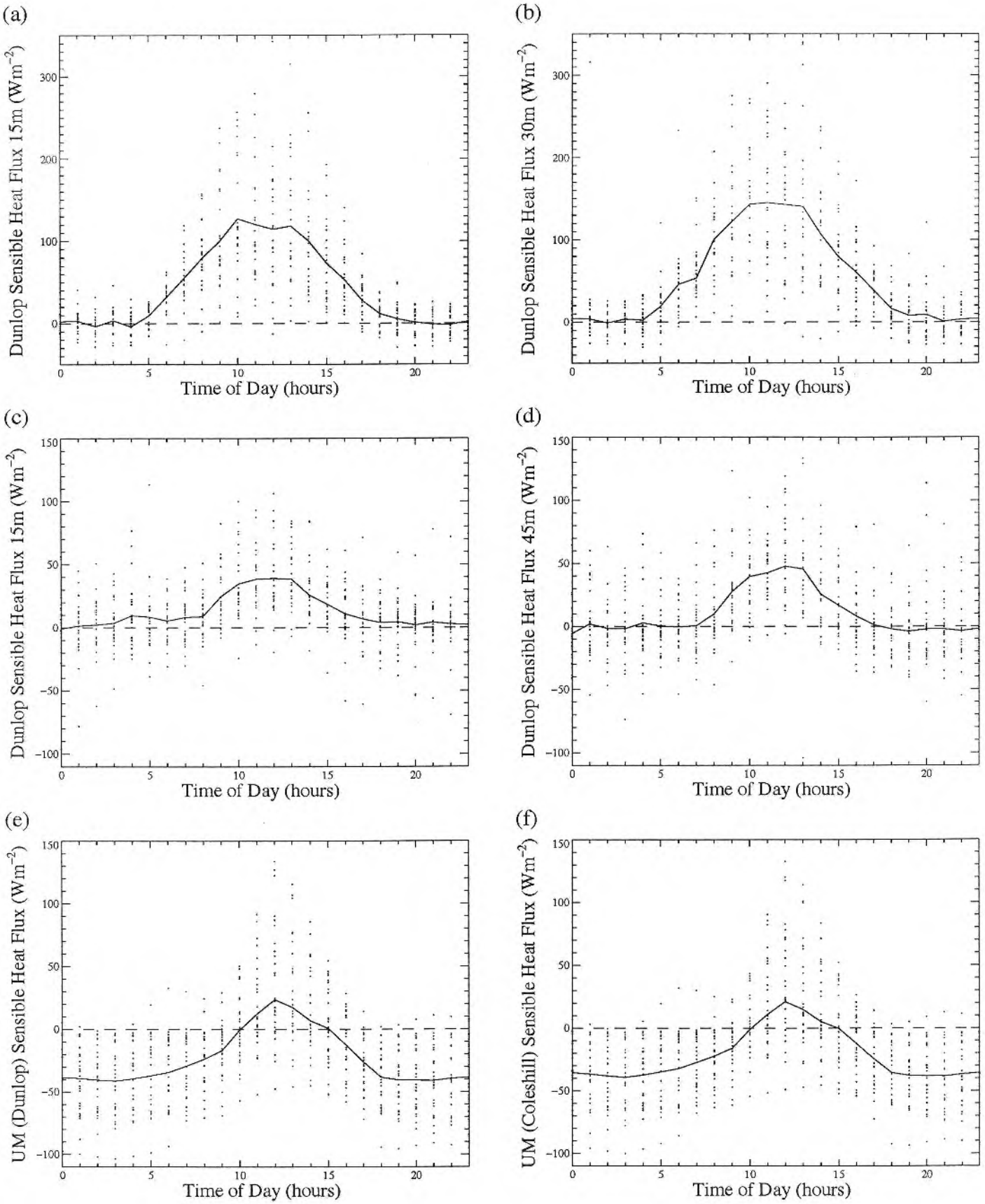

Figure 10: Scatter plots of hourly sensible heat flux values overplotted with a mean diurnal cycle, calculated by averaging over the measuring period.
(a) Dunlop 15m, 1998 data, (b) Dunlop 30m, 1998 data, (c) Dunlop 15m, 1999 data, (d) Dunlop 45m, 1999 data, (e) UM (Dunlop), 1999 data and (f) UM (Coleshill), 1 999 data

$S_{\downarrow}$	incoming shortwave radiation
$S_{\uparrow}$	outgoing shortwave radiation
$L_{\downarrow}$	incoming longwave radiation
$L_{\downarrow}^{refl}$	reflected incoming longwave radiation
$L_{\uparrow g}$	outgoing longwave radiation from ground
$L_{\uparrow s}$	outgoing longwave radiation from surface (canopy)
H	sensible heat flux
λE	latent heat flux
G	ground flux
β	fraction of radiation absorbed by the canopy.

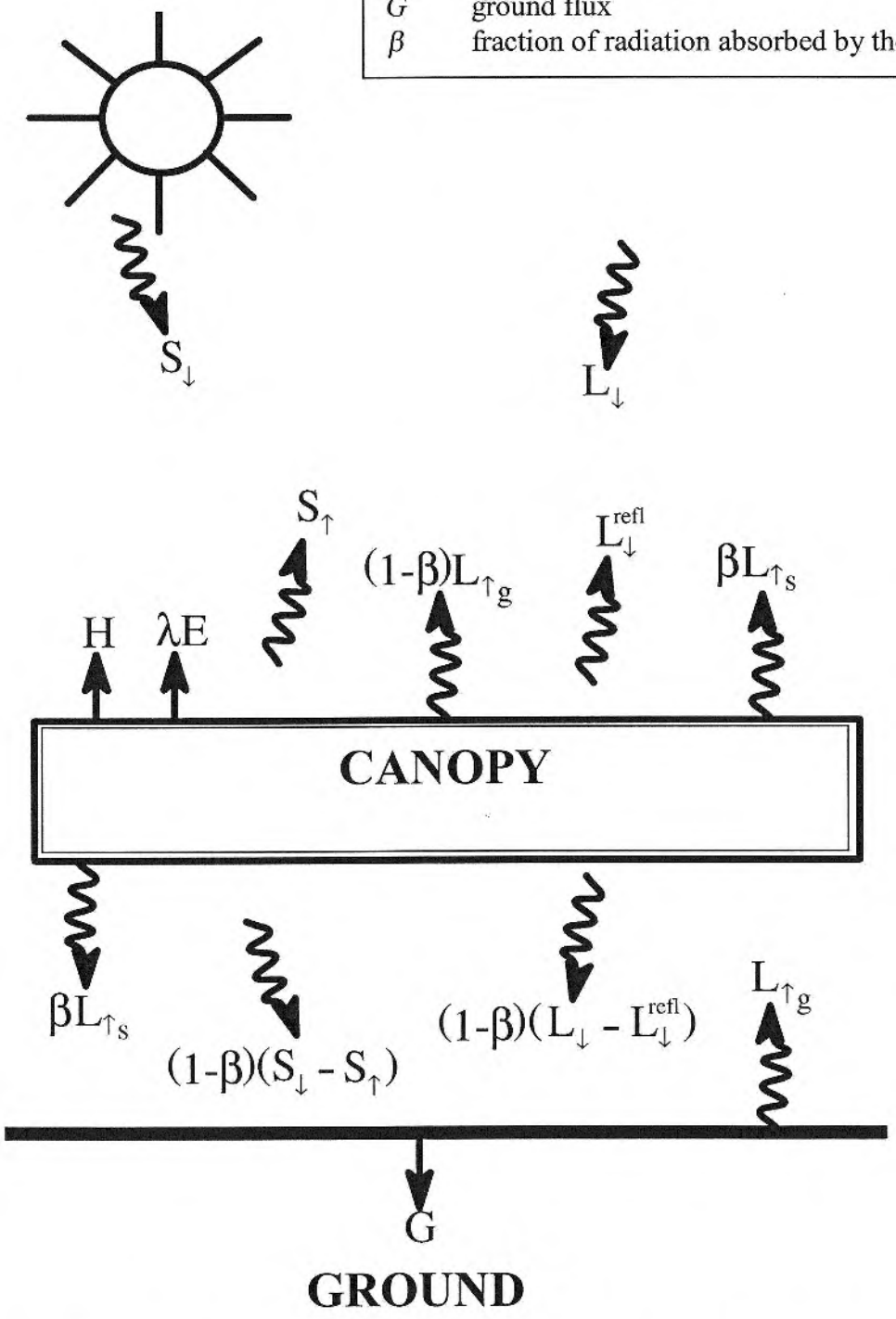

Figure 11: Terms that make up the SEB energy balance across a canopy and the energy balance at the surface below. (Best, 1998)

	Vegetation Canopy*	Concrete Canopy
Thermal Conductivity of Ground below Canopy ($Wm^{-1}K^{-1}$)	2.0	0.75 ** Asphalt
Thermal Capacity of Ground below Canopy ($Jm^{-3}K^{-1}$)	2.5×10^{6}	1.94×10^{6} ** Asphalt
Thermal Capacity of Canopy ($Jm^{-3}K^{-1}$)	1.0×10^{4}	0.28×10^{6} ** Aerated concrete
Leaf Area Index (area of leaf/unit area of ground)	4.0	1.0 *
Height of Veg/Canopy (m)	0.1	1.0
Roughness Length for Momentum (m)	0.01	1.0
Roughness Length for Temperature (m)	0.001	0.1
Surface Albedo	0.23	0.2 **
Emmisivity of Ground below Canopy	0.96	0.95 **
Emmisivity of Canopy	0.98	0.8 **
Vegetation (T/F)	T	T (to select canopy)
Road (T/F)	F	F (to select canopy)
Soil Moisture	3	0

* Martin Best, personal communication
** Oke (1990)

Table 1: Typical values for the properties of the canopy and the surface below the canopy (vegetation or concrete).

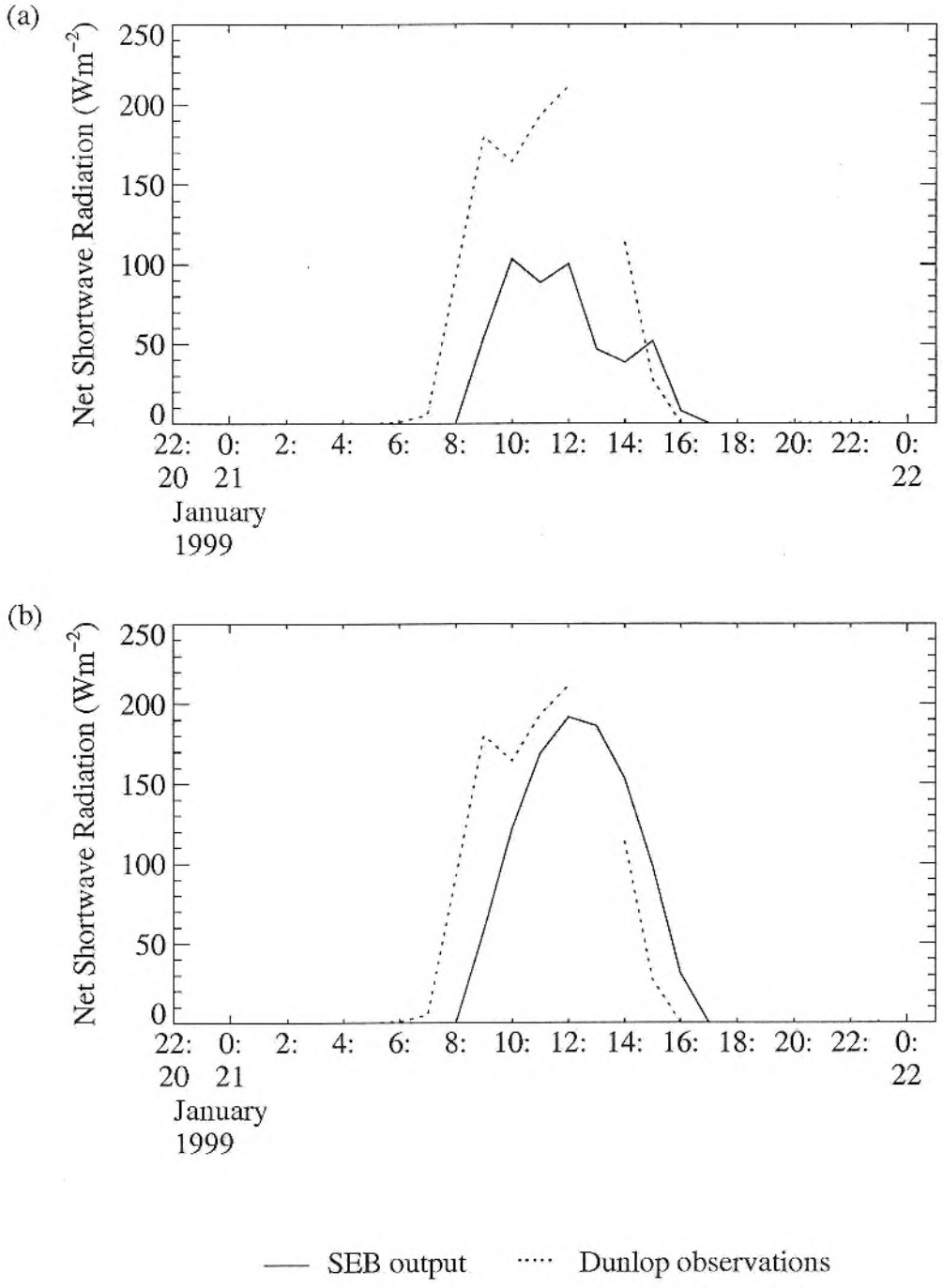

Figure 12: Net shortwave radiation for 22 January 1999. SEB run with (a) Coleshill cloud cover and (b) clear skies.

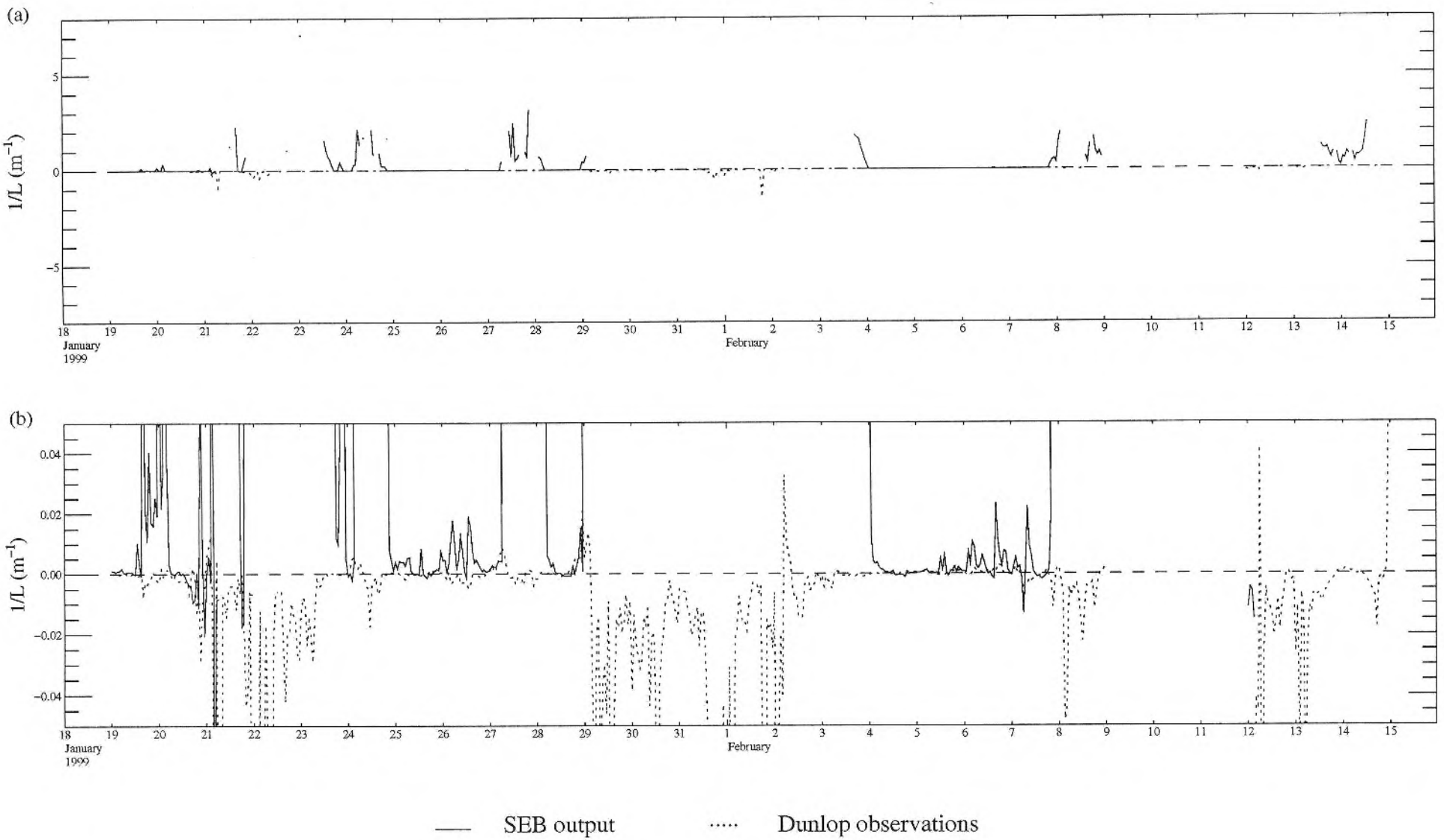

Figure 13: (a) Times series of SEB calculated 1/L overlaid with Dunlop observations.
(b) same data as in (a) but with an adjusted y–axis range.

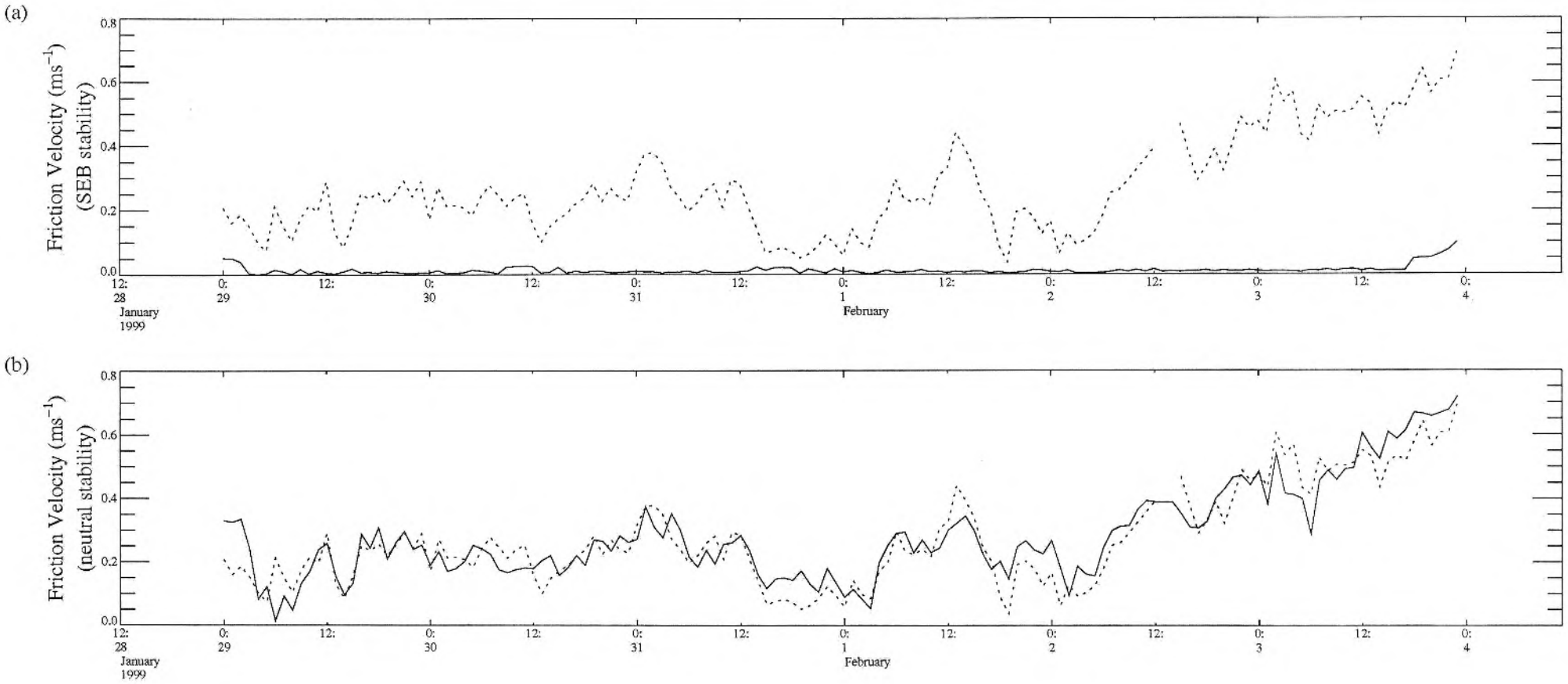

—— SEB output ····· Dunlop observations

Figure 14: Time series of friction velocity with (a) stability determined by SEB and (b) neutral stability assumed.

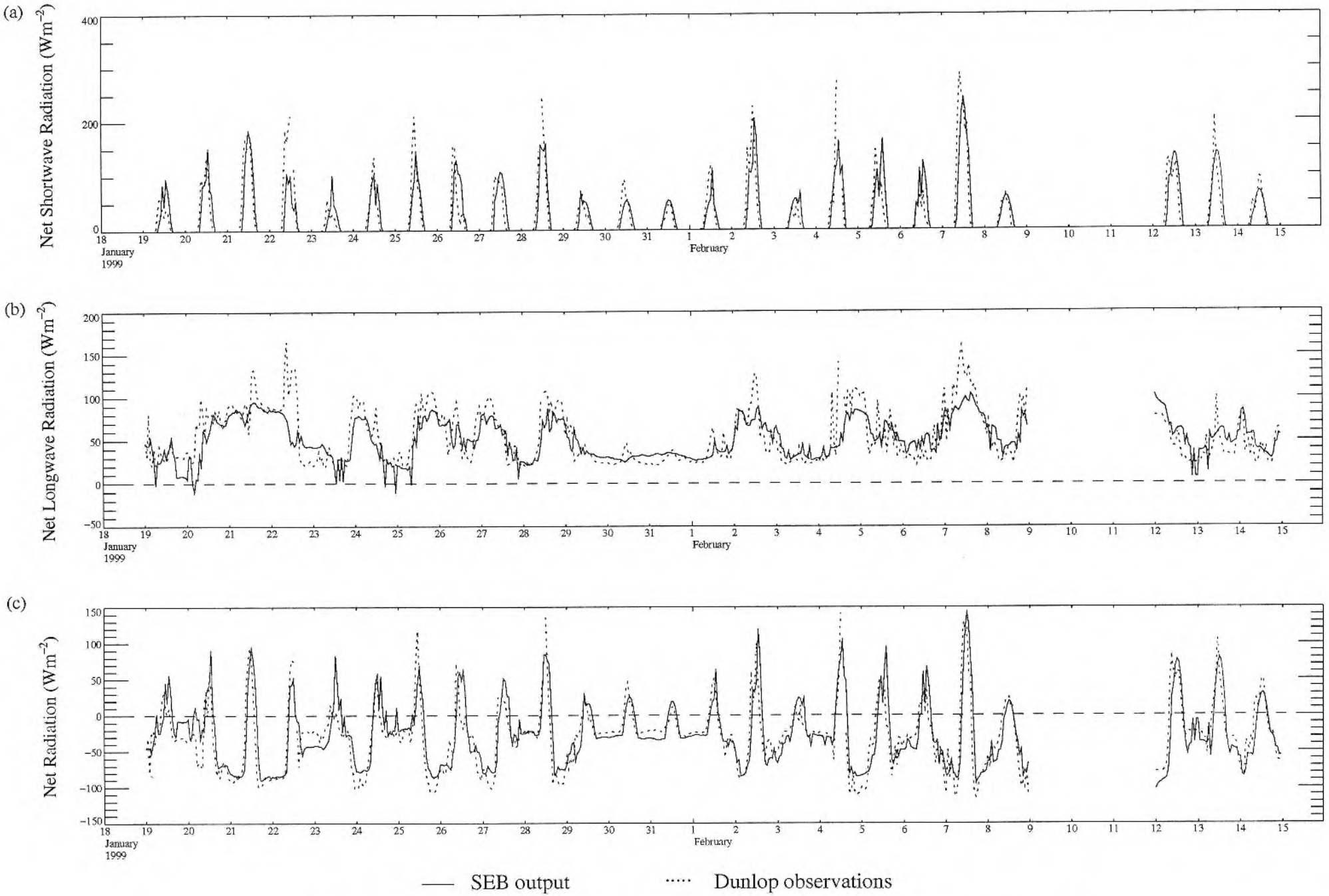

Figure 15: Time series of SEB model output overlaid with Dunlop observations. (1999 data).

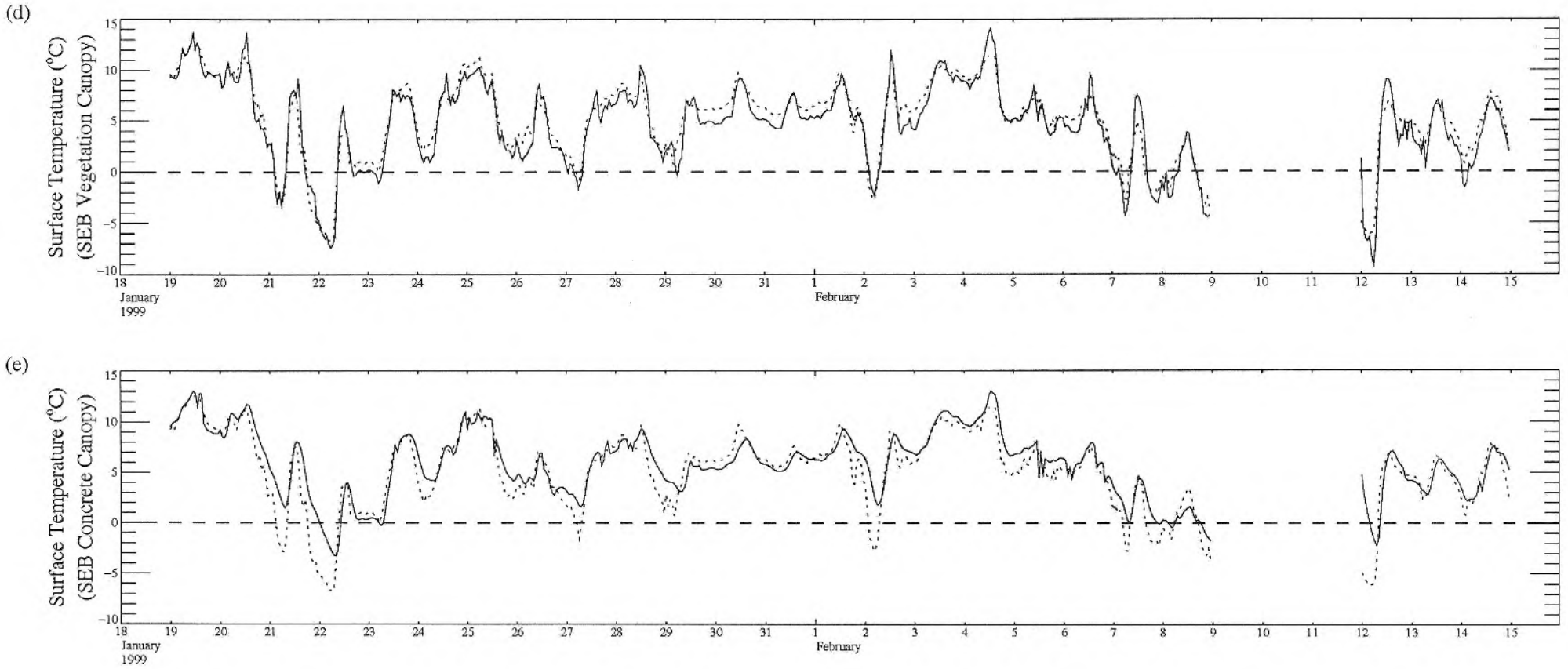

—— SEB output ····· Dunlop observations

Figure 15 contd.: Time series of SEB model output overlaid with Dunlop observations. (1999 data).

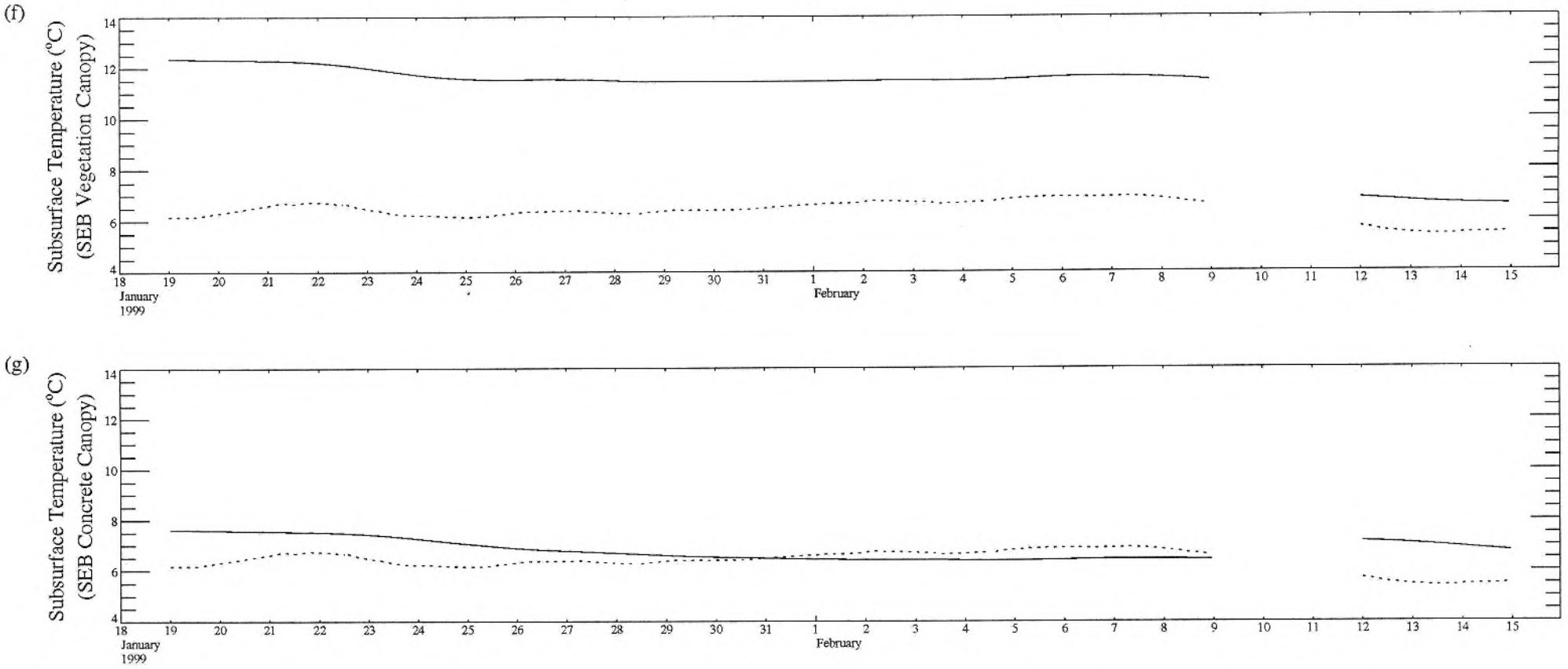

—— SEB output ····· Dunlop observations

Figure 15 contd.: Time series of SEB model output overlaid with Dunlop observations. (1999 data).

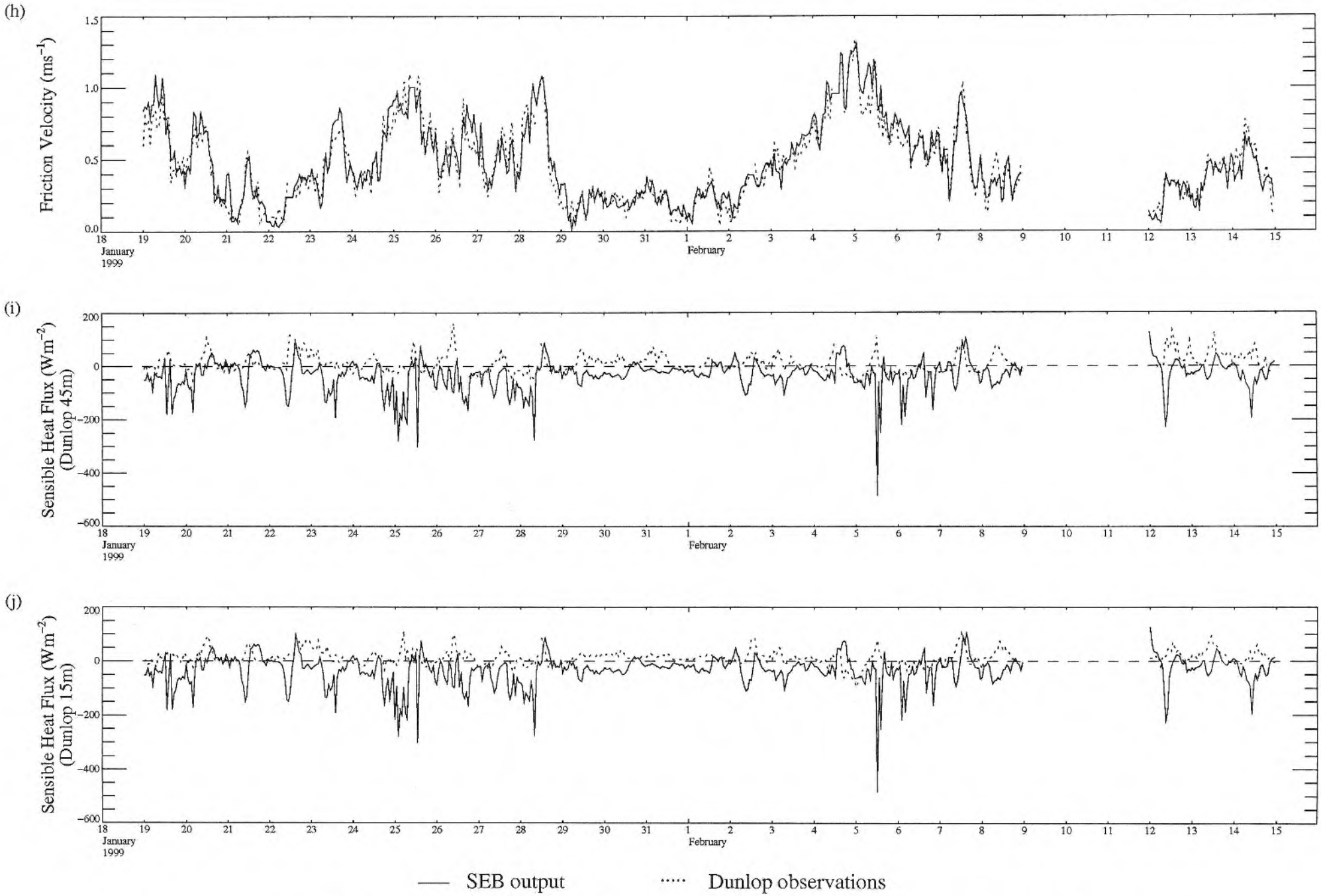

Figure 15 contd.: Time series of SEB model output overlaid with Dunlop observations. (1999 data).